Virus Research 297 (2021) 198386

Contents lists available at ScienceDirect

Virus Research

journal homepage: www.elsevier.com/locate/virusres

Short communication

Genomic and biological characterization of a novel partitivirus infecting *Fusarium equiseti*

Mathieu Mahillon [a], Alain Decroës [a], Simon Caulier [a], Assiata Tiendrebeogo [a,b], Anne Legrève [a], Claude Bragard [a,*]

[a] Earth and Life Institute, Applied Microbiology-Phytopathology, UCLouvain, Louvain-la-Neuve, Belgium
[b] Natural System, Agrosystem and Environmental Engineering, Phytopathology, Nazi Boni University, Bobo-Dioulasso, Burkina-Faso

ARTICLE INFO

Keywords:
Mycovirus
Fusarium equiseti
Partitiviridae
Zetapartitivirus
Hypovirulence

ABSTRACT

This study describes a new mycovirus infecting a strain from the *Fusarium incarnatum-equiseti* species complex. Based on phylogenetic and genomic analyses, this virus belongs to the recently proposed genus "Zetapartitivirus" in the family *Partitiviridae*. The name "Fusarium equiseti partitivirus 1″ (FePV1) is therefore suggested for this novel viral species. Similar to other partitiviruses, FePV1 genome is composed by two dsRNA segments that exhibit each one large ORF encoding for an RdRp and a CP, respectively. A smaller dsRNA was also detected in infected mycelium and could be a satellite RNA of FePV1. In addition to characterized zetapartitiviruses, other FePV1-related sequences were retrieved from online databases and their significance is discussed. Following conidial isolation, an FePV1-free isogenic line of the fungal host was obtained. In comparison with the original infected strain, this line showed higher growth, biomass production and pathogenicity on tomato, advocating that FePV1 induces hypovirulence on its host.

Plant pathogenic fungi represent a major threat to crop production worldwide, hence modern agriculture relies on the use synthetic fungicides as control measure (McDonald and Stukenbrock, 2016). Yet, ecological studies have evidenced hazardous side-effects associated with some of those molecules (Yang et al., 2011). Along with the emergence of fungicide resistance (Fisher et al., 2018), such results have raised public concerns, boosting the scientific community to develop ecologically friendly alternatives. Mycoviruses conferring hypovirulence (*i.e.* reduced virulence) to their host can be used for this purpose (Xie and Jiang, 2014). While this approach is still in its infancy, it has already been efficiently demonstrated by several studies (Yu et al., 2013).

Mycovirus-mediated hypovirulence has been investigated for members of the genus *Fusarium*. In 2002, a pioneering study has demonstrated that dsRNA mycoviruses infecting *F. graminearum* are able to reduce host growth and disease severity on grains (Chu et al., 2002). Since then, numerous novel *Fusarium* viruses have been characterized, but only a handful were shown to induce hypovirulence (Li et al., 2019), calling for more virus hunting. Most studies have been limited so far to well-characterized members of this genus. Therefore, there is a need to screen neglected species. Among those, the *F. incarnatum-equiseti* species complex (FIESC) appears to be an ideal candidate. Indeed, despites being a large group accommodating species that have been isolated from diverse sources, FIESC has been barely screened for mycoviruses, with only one alternavirus identified in a species from the clade Incarnatum (Zhang et al., 2019). Moreover, several reports have demonstrated the pathogenic nature of FIESC species towards plants as well as their production of harmful mycotoxins (Langseth, 1998), raising the need for deeper investigation on pathogenicity and control strategies.

In this context, nine FIESC strains isolated from tomato in Burkina Faso in 2018 were screened for the presence of mycoviruses by a cellulose-based dsRNA extraction protocol (Khankhum et al., 2017). In addition to fungal DNA and RNA, three bands (*ca.* 1.4–2.0 kb) with relative high intensity were observed by agarose gel electrophoresis for the strain 020FO1−18 (Fig. S1). This strain was sampled from a rotten tomato and identified as a species belonging to the clade Equiseti by partial sequencing of the EF1α gene (O'Donnell et al., 2000). The three bands were proven to be dsRNA by resistance to S1 nuclease and DNase Q1 (Fig. 1A). After treatment, the dsRNA was sent to Macrogen for Illumina Truseq sequencing. Following analysis as previously described (Mahillon et al., 2019), the three dsRNA segments were found to be 1, 823, 1583 and 1415 bp in length respectively, and their sequences were deposited in the Genbank database under accession numbers

* Corresponding author.
E-mail address: claude.bragard@uclouvain.be (C. Bragard).

https://doi.org/10.1016/j.virusres.2021.198386
Received 30 January 2021; Received in revised form 3 March 2021; Accepted 8 March 2021
Available online 11 March 2021

MT659122-MT659124.

A Blastn search in the nr database using the two longest dsRNA nucleotides as queries resulted in significant hits (>10 % cover, E-value<2e-06) corresponding to several mycoviruses (Table 1) that were recently grouped inside the proposed genus "Zetapartitivirus" from the family *Partitiviridae* (Gilbert et al., 2019). The two longest dsRNA were therefore assigned to a novel viral species for which the name "Fusarium equiseti partitivirus 1″ (FePV1) is proposed. Unlike dsRNA 1 and 2, no hit was obtained for a similar Blastn search on the smallest dsRNA. Consistent with characterized zetapartiviruses, a nucleotide analysis predicted one large ORF for both FePV1 dsRNA 1 and 2 at positions 35–1756 and 49–1494 (on the positive strand), respectively (Fig. 1B). On the other hand, no large ORF was found on the third dsRNA. Furthermore, this dsRNA does not show nucleotide similarities with the two other dsRNA, and is therefore not a defective RNA. Rather, this dsRNA might be a non-coding satellite RNA (satRNA) that requires FePV1 as helper virus (HV), as proposed for the small dsRNA associated with BdPV1 (Wang et al., 2014).

When the 5′-termini of FePV1 dsRNA were aligned with those of zetapartitiviruses, the motif CGAAAAUKMGUCACAAYAUHAYMNUUHYC (with K = G/U, M = A/C, Y = C/U, H = A/U/C) was found for FePV1, BdPV1, AtPV1 and AfuPV2 (Fig. 1C, left panel). In terms of structure, this motif was previously predicted to fold into a stable hairpin (Wang et al., 2014). The 5′-termini of DcPV1 and PbPV1 dsRNA contain mismatches and deletions with regard to this motif. Moreover, their respective dsRNA 1 show additional 5′ residues. These differences might be due to their method of identification that consisted in an analysis of fungal RNAseq data (Gilbert et al., 2019), limiting the identification of actual termini due to a lower sequencing depth. The 5′-termini of BdPV1 and AtPV1 are more reliable since they have been obtained by amplicon-based methods. The 5′-terminus of FePV1 satRNA shows some similarity to the conserved motif, as described for BdPV1 satRNA, which is an usual characteristics of satRNA towards their HV (Huang et al., 2010).

Unlike the 5′-termini, an analysis of the 3′-termini for all aforementioned viruses did not reveal such a large motif, as already observed by another study (Zoll et al., 2018). Yet, the short motif UCAUUA was found to be conserved in this region for the dsRNA of FePV1 and all other zetapartitiviruses (Fig. 1C, right panel). Slightly different motifs with one mismatch each were detected in this region for both satRNA. Using the RNA folding form on the Mfold web server (Zuker, 2003), the 3′-termini of FePV1 dsRNA 1, 2 and satRNA were predicted to fold into stable structures containing 2–3 hairpins (Fig. 1D). Interestingly, the conserved motif is found in loops of hairpin for each dsRNA (Fig. 1E, obtained using Forna (Kerpedjiev et al., 2015)), an observation already made for BdPV1 (Wang et al., 2014).

The large ORF of FePV1 dsRNA 1 putatively encodes for a protein of 574 aa (estimated mass Mr = 65.2 kDa). A Blastp search for this protein in the nr database resulted in significant hits (99 % cover, E-value = 0) corresponding to RNA-dependent RNA-polymerase (RdRp) from the characterized zetapartitiviruses. Those proteins are highly similar in size (569–574 aa) and exhibit a conserved RdRp domain (pfam00680), which is also found in FePV1 protein at position 191–485 (E-value = 1.86e-14). In this domain, the conserved motifs A–G (Bruenn, 2003) were readily identified (Fig. S2). Notably, zetapartitiviruses RdRp show <66 % aa identities with FePV1 RdRp, which is lower than the threshold for species demarcation in this family (90 %, (Vainio et al., 2018)), confirming that FePV1 should be considered as a new species.

To date, five genera of *Partitiviridae* have been recognized by the International Committee on Taxonomy of Viruses (ICTV): *Alpha-*, *Beta-*, *Gamma-* and *Deltapartitivirus* and *Cryspovirus* (Vainio et al., 2018). In terms of host range, members of the first two genera have been found in plants, ascomycetes and basidiomycetes. Gammapartitiviruses were found in ascomycetes and recently in a species of the phylum Oomycota

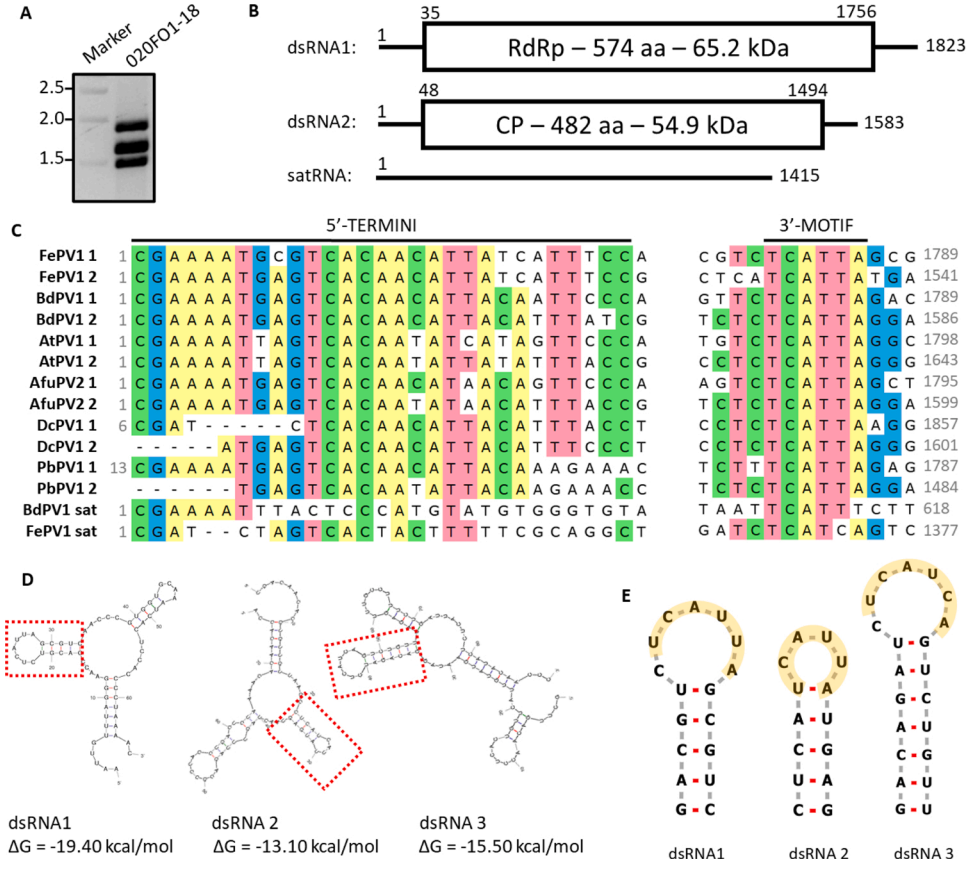

Fig. 1. Description of FePV1 dsRNA 1-2 and its putative satRNA (**A**) Electrophoresis agarose (1%) gel showing the three dsRNA purified from the strain 020FO1-18 and treated with DNase I and S1 nuclease. Marker: Promega 1 kb ladder. Numbers on the left refer to as selected DNA weight markers expressed in kb. (**B**) Schematic representation of FePV1 genome. Each dsRNA is represented by a horizontal line. Relevant nucleotide positions (start, end and ORF) are indicated. Boxes represent large ORF with associated protein function, size and weight. (**C**) Left : cDNA alignment for the 5′-termini of dsRNA of FePV1 and other zetapartitiviruses and satRNA. Right : the conserved motif found in proximity to the 3′-termini for the same dsRNA. Nucleotides with colored background are present in at least 50 % of the sequences. Nucleotides positions are indicated next to the sequences. **(D)** Structural prediction for the 3′-termini of FePV1 dsRNA 1, 2 and satRNA with associated minimal energy. The hairpin containing the conserved motif is highlighted by dotted red boxes. (**E**) Hairpins containing the conserved motif (orange background) for FePV1 dsRNA 1, 2 and satRNA.

Table 1
General features of characterized zetapartitiviruses nucleotides and associated satRNA.

Virus name	Segment number	Accession number	Size (bp)	5′UTR (bp)	3′UTR (bp)	ORF (aa)	Ref.
Alternaria alternata partitivirus 1 (AtPV1)	1	KY352402	1833	34	83	571	(Xavier et al., 2018)
	2	KY352403	1680	71	103	501	
Botryosphaeria dothidea partitivirus 1 (BdPV1)	1	KF688740	1823	35	70	572	(Wang et al., 2014)
	2	KF688741	1623	52	87	494	
	satRNA	KF688742	682	–	–	–	
Aspergillus fumigatus partitivirus 2 (AfuPV2)	1	MH192991	1822	34	66	573	(Zoll et al., 2018)
	2	MH192992	1638	95	91	483	
Penicillium brasilianum partitivirus 1 (PbPV1)	1	MK279470	1791	58	23	569	(Gilbert et al., 2019)
	2	MK279471	1518	24	132	453	
Delitschia confertaspora partitivirus 1 (DcPV1)	1	MK279446	1899	94	90	571	
	2	MK279447	1645	50	90	501	
Fusarium equiseti partitivirus 1 (FePV1)	1	MT659122	1823	34	64	574	This study
	2	MT659123	1583	48	138	482	
	satRNA	MT659124	1415	–	–	–	

(Shiba et al., 2018). Deltapartitiviruses have been found in plants (Wu et al., 2020) and very recently in an ascomycete (Zhang et al., 2020). The unique cryspovirus infects a chromist from the phylum Apicomplexa (Nibert et al., 2009). In recent years, dozens of new putative partitiviruses have been detected in various samples by (meta)viromics studies. In particular, a high diversity of such viruses was discovered in invertebrates (Shi et al., 2016). Galbut virus, a new partitivirus found in *Drosophila melanogaster*, was shown to infect fly cells, giving strong evidences for this unexpected new host range (Cross et al., 2020). Novel partitiviruses with distinct RdRp were also discovered in fungi, leading to the proposition of two new genera, namely "Epsilsonpartitivirus" and thus "Zetapartitivirus" (Gilbert et al., 2019) that still need approval by the ICTV. RdRp of partitiviruses are related to those of other groups of dsRNA viruses: the family *Amalgaviridae* (Sabanadzovic et al., 2009) and the proposed mycoviral groups "Urniviridae", "Ustivirus" and "Bipartitevirus" (Herrero, 2016; Kotta-Loizou and Coutts, 2017; Nerva et al., 2016). Those taxa are more distantly related to the family *Picobirnaviridae* that accommodates dsRNA viruses presumably infecting animal-associated prokaryotes (Krishnamurthy and Wang, 2018).

In order to get insight on the phylogenetic placement of FePV1, the aa sequence of its RdRp was aligned using Muscle (Edgar, 2004) with those of other zetapartitiviruses as well as other representative viruses from the aforementioned groups (see Fig. 2 for accession numbers). The best fit substitution model (VT + F+I + G4) for this alignment was retrieved via ModelFinder (Kalyaanamoorthy et al., 2017) and used to create a phylogenetic tree using IQ-Tree (Nguyen et al., 2015) in combination with ultrafast bootstrap (Hoang et al., 2018). The obtained tree was then visualized and cured using iTOL (Letunic and Bork, 2019). In this tree (Fig. 2), FePV1 and other zetapartitiviruses form a strongly supported monophyletic clade inside the family *Partitiviridae*. With less

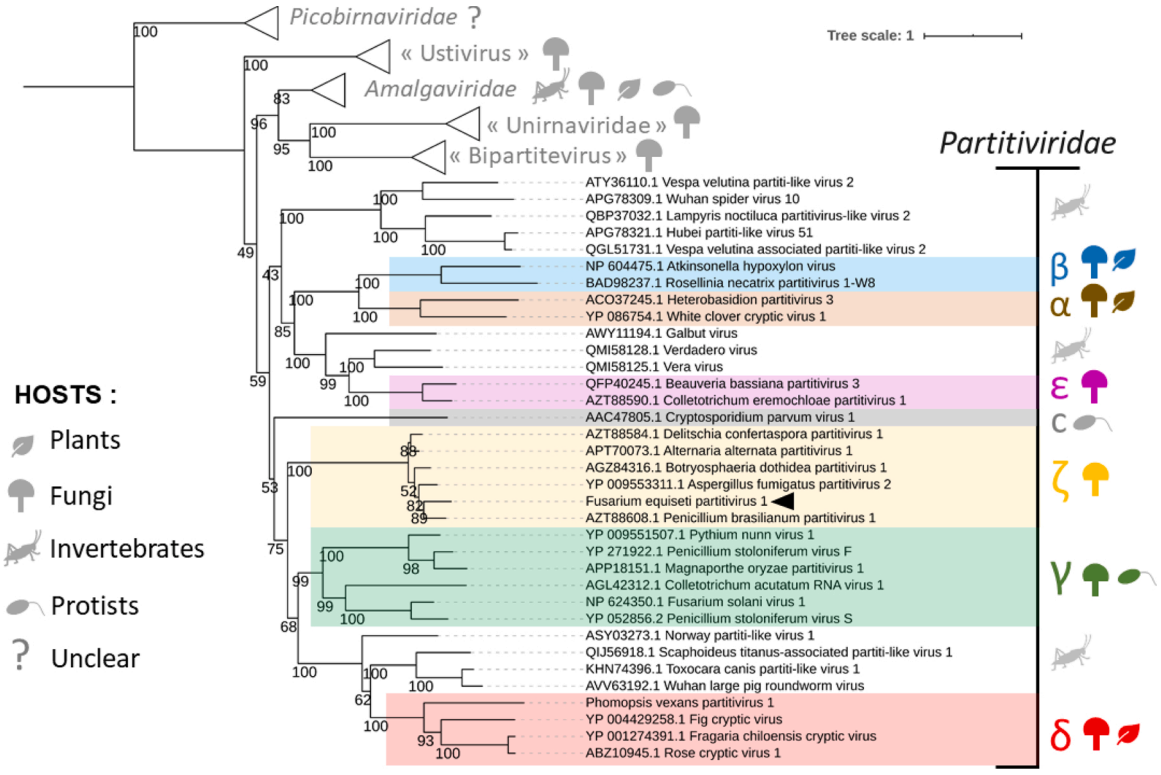

Fig. 2. ML phylogenetic tree based on an alignment of RdRp of zetapartitiviruses and related viruses. The tree scale is given in substitution per site. Accession numbers of proteins are given next to virus names. Numbers on the nodes give the percentage of bootstrap replicates that groups the branch together. The black arrow indicates the position of FePV1 RdRp in the tree. RdRp of Otarine and Human picobirnavirus (members of Picobirnaviridae) were taken to root the tree. Colored boxes represent Partitiviridae genera as indicated by greek letters: Alpha- (α), Beta- (β), Gamma- (γ), Delta- (δ), Epsilon- (ε) and Zeta- (ζ) except for Cryspovirus (c).

support, this tentative genus groups together with *Cryspovirus*, *Gammapartitivirus*, *Deltapartitivirus* and several unclassified invertebrate-associated partitiviruses.

In addition to characterized zetapartitiviruses, several predicted viral RdRp from (meta)viromics studies were obtained by different Blast searches on FePV1 sequences. Indeed, a Blastn search on FePV1 dsRNA 1 yielded significant hits (Table S2) related to contigs obtained from Californian grassland soils (Starr et al., 2019), feces of fruit bats in Cameroon (Yinda et al., 2018) and mycelia from *Plasmopora viticola* collected in Italy and Spain (Chiapello et al., 2020). Furthermore, a Blastp search on FePV1 RdRp yielded additional significant hits (Table S3) corresponding to contigs obtained from marine microorganisms sampled in surface water from the Pacific ocean (Urayama et al., 2018) and lichen from Japan (Urayama et al., 2020). A phylogenetic analysis of all those RdRp showed that several can be placed within "Zetapartitivirus" (Fig. S3). Due to their methods of identification, the actual host of those putative new zetapartitiviruses is not defined. Nevertheless, "Plasmopara viticola lesion associated Partitivirus 2″ (PVaPartit2) could be an exception since its contigs were detected from mycelia collected in different locations, advocating that it represents an actual virus of this oomycete.

The large ORF detected on FePV1 dsRNA 2 putatively encodes for a protein of 482 aa (Mr =54.9 kDa). A Blastp search for this protein in the nr database evidenced significant hits (>88 % cover, E-value≤9e-146) corresponding to proteins encoded by the dsRNA 2 of other zetapartitiviruses. In the case of BdPV1, this protein was associated with virions, leading to its assignment as the CP (Wang et al., 2014). This role can also be assigned for other zetapartitiviruses dsRNA 2-encoded proteins because of similarities in sizes (453–501 aa) and high percentages (50–65 %) of pairwise identities (Fig. 3A, obtained using SDT software (Muhire et al., 2014), see Table S4 for accession numbers). Those CP showed <34 % pairwise identities with CP from other *Partitiviridae* genera (Fig. 3A), highlighting that both RdRp and CP from zetapartitiviruses are distinct in the family.

In order to visualize the particles of FePV1, a purification protocol based on a sucrose density gradient (Sasaki et al., 2005) was followed. Samples containing purified particles were then applied on a carbon-coated 200 mesh-nickel grid (Agar scientific). Next, the grid was observed by transmission electron microscopy (TEM) using the TECNAI G^2 20 LaB6 at 80 kV. Isometric particles (*ca.* 35 nm in diameter) were detected (Fig. 3B), consistent with similar studies performed for BdPV1 and AtPV1 (Wang et al., 2014; Xavier et al., 2018).

A similarity plot of zetapartitiviruses CP sequences (obtained using https://www.bioinformatics.nl/cgi-bin/emboss/plotcon, with window size = 20) showed that the N-ter region is highly variable (Fig. 3C). Structural predictions (Fig. 3D, obtained using Jalview (Waterhouse et al., 2009)) showed that this region is likely disordered. This prediction was already made for the CP of *Penicillium stoloniferum virus S* and *F* (Tang et al., 2010). For those viruses, the CP N-ter region presumably localizes inside mature virions where it interacts with viral nucleotides via positively charged aa. Likewise, this region is rich in lysine (K) and arginine (R) residues for all zetapartitiviruses (Fig. S4). Downstream of the N-ter extremity, zetapartitiviruses CP show two relatively conserved regions rich in α-helices separated by a highly variable central region (Fig. 3C and D). This structural organization reminds the shell-arch-shell domains described for 3D-characterized partitiviruses (Nibert et al., 2013). Shell domains interact with each other and are necessary for the integrity of viral particles, while the arch domain is exposed to the particle surface and is arguably less constrained in terms of sequence.

When the (meta)viromics datasets associated with the putative novel zetapartitiviruses were screened for the presence of FePV1 CP homolog, only one hit was obtained from the marine microorganisms virome (GBH21831.1, 490 aa, E-value = 4e-175), reinforcing the idea that an actual zetapartitiviruses was detected in that study. Curiously, two dsRNA exhibiting large ORF were associated with the RdRp-encoding dsRNA of PVaPartit2 but none of these encodes for homolog of FePV1 CP. Rather, a Blastp search on the first protein (QHD64794.1) showed that it is similar to CP from alphapartitiviruses (for example, the CP of Rosellinia necatrix partitivirus 5 was found in the hits with 79 % cover and E-value = 4e-33). A Blastp search on the second predicted protein

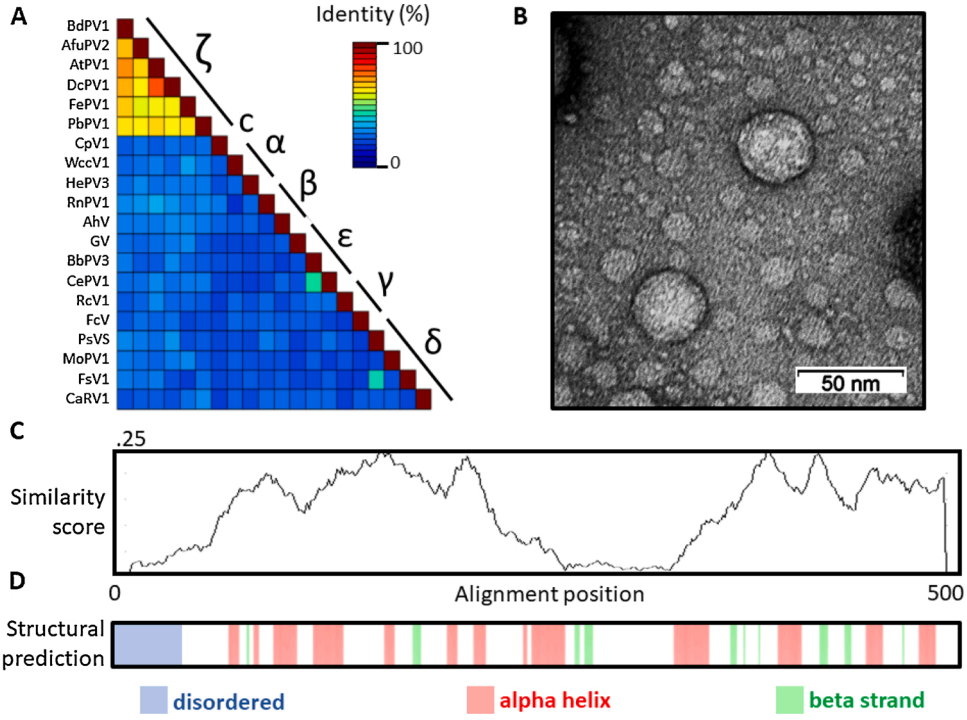

Fig. 3. FePV1 CP characterization. (**A**) Pairwise identity matrix for CP of zetapartitiviruses and representative members of other partitiviral genera. See Table S4 for complete viral names and accession numbers; (**B**) Isometric viral particles visualized by TEM; (**C**) Similarity plot of an alignment of zetapartitivuses CP. **(D)** Predicted secondary structures for FePV1 CP.

(QHD64806.1) resulted in hits corresponding to proteins with unknown function encoded by gammapartitiviruses (for example, a protein from Aspergillus fumigatus partitivirus 1 was found with 62 % cover and E-value = 2e-21). At this point, it is unclear whether the assignment of those three dsRNA into a single viral genome is an artefact or it corresponds to an actual virus that resulted from the reassortment of different partitiviruses.

Previously, a protein homologous to that of BdPV1 CP was evidenced in the genome of *Exophiala dermatitidis* (Wang et al., 2014). Interestingly, following a Blastp search on FePV1 CP in the nr database, this homolog was obtained again, but four additional significant hits were also listed corresponding to predicted proteins from two other ascomycetes and one diatom (Table S4). These viral sequences found in eukaryotic genomes could be endogenous viral elements (EVEs), *i.e.* reliquats of ancestral viruses that have integrated into their host DNA during horizontal gene transfer (HGT). A similar Blastp search on FePV1 CP was performed in other NCBI databases but no additional significant hit was found. To extend further the analysis, the same query was used for tBlastn searches. In the whole genome shotgun (wgs) database, this search yielded 51 significant hits related to genomes of ascomycetes and an additional diatom (Table S5).

The coding potential of these putative EVEs is quite diverse. Several EVEs exhibit almost intact ORF with size and sequence highly similar to FePV1 CP, indicating a relatively recent HGT. This is the case for EVEs detected from members of the genera *Fusarium* (Meena et al., 2018; Proctor et al., 2018), *Exophilia* (Song et al., 2020), *Wickerhamiella* (Gonçalves et al., 2018; Shen et al., 2018) and *Suhomyces* (Shen et al., 2018). Other EVEs showed shortened ORF disrupted by premature stop codon and frameshifting. Those were found in members of the genera *Neurospora* (Gioti et al., 2013), the *Symbiotaphrina buchneri* strain JCM 9740 and the *Lipomyces japonicus* strain NRRL Y-17,848 (Shen et al., 2018). For the latter, two other EVEs were evidenced in different genomic locations, but they are apparently non-coding due to absence of proper initiation codon. Likewise, no ORF could be found for the EVE present in the *Dicyma pulvinata* strain 414−3 (Sushida et al., 2019).

Curiously, some EVEs seem to be part of ORF significantly longer than FePV1 CP (Fig. S5). This is the case for two EVEs found in the *F. longipes* strain NRRL 20,695 (Proctor et al., 2018) that are present in distinct genome locations. The first EVE is part of an ORF for which the predicted protein contains an N-ter heterokaryon domain (HET, pfam06985). The second EVE is located in an ORF for which the predicted protein shows high similarities with proteins from other *Fusarium* species. Other examples of EVEs placed in long ORF are those found in several *Starmeralla* species. On some of those ORFs, conserved domains were detected. For example, on the ORF found in the *S. sorbosivorans* strain CBS 8768, a Sec24-related protein domain (PTZ00395) was found. However, in that case the ORF does not exhibit proper stop codon and is located at the end of a contig. On two other ORFs found in strains of *S. apicola*, the FePV1 CP homology appears to be split in different parts and a *herpesvirus* major outer envelope glycoprotein domain (pfam05109) is found between CP moieties. The last type of EVEs being part in long ORF are those found in the genomes of the *Pseudo-nitzschia multistriata* strain B856 and the *Nitzschia* sp. strain Nitz4. In that case, the FePV1 CP homology is found in the C-ter region of two large predicted proteins, whereas their N-ter contain a *herpesvirus* transcriptional regulator protein ICP4 consensus domain (PHA03307). Additionally, on the EVE the latter, a conserved DNA excision repair protein domain (TIGR00600 or rad2) was found. When the FePV1 CP was used a query for a tBlastn search, a partial transcript for this ORF was found (Table S7). Furthermore, two other similar long proteins could be detected in transcripts of the *N. palea* strain CPCC-160 and the *Nitzschia* sp. strain ChengR-2013. Notably, those proteins exhibit the already mentioned domains pfam05109 and PHA03307. Another common and intriguing characteristics for those proteins is the presence of many serine residues (18–23 % of total amino acids content). Additional partial transcripts related to those ORFs were detected from the latter strains and from the *Cylindrotheca closterium* strain CS-5.

Besides diatoms, sequences related to FePV1 CP were also found in other eukaryote transcriptomic data. A transcript from the chytrid *Piromyces* sp. E2 (GT900911.1, 35 % coverage, E-value = 6e-18) was found by a tBlastn search in the expressed sequence tag (EST) database. No similar hit was found in the genome of this chytrid, advocating that the transcipt corresponds to the partial sequence of an actual zetapartitivirus. Yet, no RdRp homolog was found in the same dataset. Two additional hits were found from the transcriptome shotgun assembly (TSA) database of the wasp *B. neomexicana* and the plant *S. bryopteris* (Table S7). Notably, when the SRA data associated with those TSA hits were screened for the presence of FePV1 RdRp homolog, such sequences were found for both datasets (Fig. S6), strongly suggesting that actual zetapartitiviruses were detected. However, as for viromics data, the host status should be taken with caution.

First discovered in asympatomatic plants, partitiviruses were traditionally considered as cryptic, persistent viruses (Nibert et al., 2014). Yet, this view is changing as several members of this family were shown to induce hypovirulence in fungi (Kamaruzzaman et al., 2019; Xiao et al., 2014; Zheng et al., 2014). When it comes to zetapartitiviruses, only BdPV1 and AtPV1 have been biologically evaluated (Wang et al., 2014; Xavier et al., 2018). BdPV1 was found in an hypovirulent strain in co-infection with a chrysovirus. No effect was associated with BdPV1 alone, while co-infection with the chrysovirus induces hypovirulence. Interestingly, authors were unable to transfer the chrysovirus into another strain without BdPV1, leaving open the possibility that the hypovirulence is the result of a synergistic interaction. In parallel, AtPV1 was discovered in a fungal strain exhibiting unusual morphological plasticity. Yet, in that case, the host could not be cured from the virus, preventing any robust conclusions.

With the aim to decipher the biological impact of FePV1, the original virus-infected strain 020FO1−18 (“Vi”) was compared with an isogenic line free of virus (“Vf”) that was obtained by conidial isolation (Mahillon et al., 2020). Absence of FePV1 was first demonstrated by dsRNA analysis (Fig. 4A). Then, both lines were analyzed by RT-PCR (Fig. 4B) using a classical protocol (Mahillon et al., 2020) in combination with primer pairs listed in Table S1. In terms of morphology, Vf colonies exhibited more aerial mycelium and a reduced sectoring tendency after 6 days on PDA in comparison to Vi colonies (Fig. 4C). Furthermore, Vf colonies exhibited a faster growth as illustrated by an average increase of 129.6 % in mycelium area (Fig. 4D). In order to compare the biomass production, 50 mL of malt extract 2% (w/v) was inoculated with 1 mL of a conidia suspension (10^4 conidia/mL) and incubated for 10 days at 22 °C in darkness, with shaking at 150 rpm. The produced mycelia were collected by filtering at 100 µm, then dried under laminar flow and eventually weighted. Results showed that the dried mass produced by the Vf line was 34.5 % higher in average (Fig. 4E). For the estimation of conidiation level, mycelia plugs were incubated seven days in 10 mL of carboxymethyl cellulose liquid medium at 30 °C with shaking at 100 rpm. The produced conidia suspensions were then filtered twice at 100 µm. Next, the concentration of conidia was estimated using a Thoma cell counting chamber. This experiment did not evidence significant difference (Fig. 4F), suggesting that FePV1 does not impact the conidiation level.

Finally, a pathogenicity assay on tomato fruit was performed according to a previously described protocol (Urban et al., 2003), with some modifications. First, commercial tomato fruits were disinfected by immersion for 30 s in ethanol 70 % (v/v) followed by three washing in sterile water. Fruits were subsequently wounded using a sharp sterile needle and 5 µL of conidia suspension (10^4 conidia/mL) were inoculated on wounds. Fruits were then placed at 22 °C with a photoperiod of 12/12 h in a sealed plastic box (30 × 30 × 40 cm) containing 40 mL of sterile water. Fungal areas were then analyzed after 6 and 14 days (Fig. 4G) using ImageJ (Schneider et al., 2012). Six days after inoculation, an average of 0.19 cm^2 of mycelium area was visible on fruits inoculated with Vf conidia (Fig. 4H). On the other side, fruits inoculated

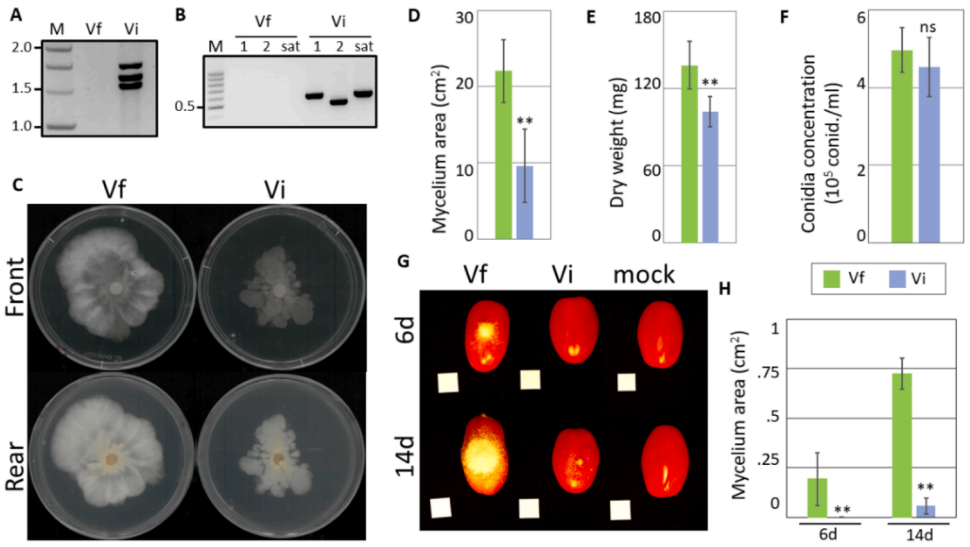

Fig. 4. Biological characterization of FePV1. (**A**) Agarose gel electrophoresis showing the dsRNA purified from the virus-free line (Vi) or the originally virus-infected line (Vi). M: Promega 1 kb ladder. Numbers on the left refer to selected DNA weight markers expressed in kb ; (**B**) Electrophoresis agarose gel showing amplicons obtained from Vf or Vi following an RT-PCR targeting FePV1 dsRNA 1, 2 and satRNA (sat). M: Promega 100 bp ladder. Numbers on the left refer to as selected DNA weight markers expressed in kb; (**C**) Typical front and rear view of mycelia produced by Vf and Vi colonies on PDA plates; (**D**) Mycelium area for Vf or Vi (n = 7); (*E*) Dry weight produced for Vf or Vi (n = 6) in liquid media; (**F**) Concentration of produced conidia for Vf or Vi (n = 10); (**G**) Tomato fruits inoculated with buffer alone (mock) or containing conidia from Vf or Vi. The white square represent 0.25 cm^2 ; (**H**) Mycelium area for Vf or Vi on inoculated tomato fruit (n = 8). For each graph, green chart represent Vf data while blue charts represent Vi data. Double asterix indicates significant difference ($p < 0.01$) while ns indicates non significant difference (Student's t-test).

with Vi conidia did not exhibit visible mycelium, similar to mock (buffer-inoculated) fruits. After 14 days, Vf mycelia had grown considerably with an average area of 0.72 cm^2. At that time point, several fruits inoculated with Vi conidia started to show mycelia, with an average area of 0.06 cm^2. Those results suggest that FePV1 delays the development of its fungal host on fruit.

Some mycoviruses can be transmitted from one host to another during anastomosis occurring by fusion of mycelia (Ghabrial et al., 2015). This mode of horizontal transmission has been efficiently used to transfer mycoviruses between *Fusarium* species (Yao et al., 2020). In addition, this ability has been demonstrated for several partitiviruses (Vainio et al., 2010; Xiao et al., 2014). In order to check whether this could also be the case for FePV1, the strain 020FO1−18 was grown on PDA next to the *F. equiseti* strain MUCL55349, the *F. incarnatum* strain MUCL55350, the *F. graminaerum* strain Fg167 and the *F. redolens* strain A63−1. Ten days after co-culture, mycelia from the receptor strains near the margin were inoculated onto fresh PDA plates. The produced mycelia were then screened for the presence of FePV1 by RT-PCR analysis as already described. None of the tested samples (performed in duplicates) gave positive signal for the virus (Fig. S7), implying the non-transfer of FePV1.

In conclusion, our study described FePV1, a new partitivirus infecting *F. equiseti*. This new virus is a bisegmented dsRNA mycovirus that can be classified in the tentative genus "Zetapartitivirus" pending official recognition. Members of this group share highly similar RdRp that are phylogenetically distinct in the family *Partitiviridae*. They also share similar CP that show predicted structural features resembling those described for 3D-characterized partitiviruses. So far, virions of zetapartitiviruses were observed by TEM. Cryoelectron microscopy is therefore expected in future studies as this technology will enable analysis at higher resolution. Other distinctive features of zetapartitiviruses have been pointed out such as the lengths of dsRNA and associated proteins (Xavier et al., 2018). Here, we also highlighted specific conserved motifs in the 5′-termini and 3′-region, both not found in other genera (Nibert et al., 2014). To date, in addition to FePV1, only six other zetapartitiviruses have been identified, infecting exclusively ascomycetes. This host range is supported by the identification of EVEs in many ascomycetous species, suggesting past infection events. Yet, more members likely exist according to (meta)viromics data, and there are also evidences that other type of organisms could be host. At this point, FePV1 could not be transferred to another strain, limiting clear biological characterization. Absence of physical contact and vegetative incompatibility between fungal strains are likely the factors limiting the transfer. Several solutions exist to solve this issue. Zinc compounds were shown to increase hyphal anastomosis and decrease incompatibility in *Rosellinia necatrix*, allowing transmission of mycoviruses (Ikeda et al., 2013). Alternatively, protoplast fusion has been efficiently demonstrated for the transfer of mycovirus between vegetative incompatible *Fusarium* species (Lee et al., 2011). Another method that avoids the use of the initial host consists in the transfection of purified viral particles, as already shown for several partitiviruses (Telengech et al., 2020). Those techniques are currently being tested and will help to enhance the biological characterization of FePV1.

Funding

This work was supported by the National Fund for Scientific Research (FNRS), UCLouvain and the Walloon Region (Antagonist project, DG03-DD-RD-R2017).

Author statements

AT performed initial fungal sampling. MM performed virus purification and particles analysis. MM and AD performed bioinformatics analyses. MM and SC performed biological analyses. MM wrote the initial draft manuscript. AD, CB, SC and AL reviewed the manuscript.

Acknowledgments

We would like to thank Charlotte Liénard, Marie Goormans, Cony Decock and Philippe Charue for technical assistance on fungi handling. We also thank Joseph Nader and Jean-Francois Colomer for their help regarding purification and observation of viral particles.

Appendix A. Supplementary data

Supplementary material related to this article can be found, in the online version, at doi:https://doi.org/10.1016/j.virusres.2021.198386.

References

Bruenn, J.A., 2003. A structural and primary sequence comparison of the viral RNA-dependent RNA polymerases. Nucleic Acids Res. 31, 1821–1829.

Chiapello, M., Rodríguez-Romero, J., Ayllón, M.A., Turina, M., 2020. Analysis of the virome associated to grapevine downy mildew lesions reveals new mycovirus lineages. Virus Evol. 6 https://doi.org/10.1093/ve/veaa058.

Chu, Y.-M., Jeon, J.-J., Yea, S.-J., Kim, Y.-H., Yun, S.-H., Lee, Y.-W., Kim, K.-H., 2002. Double-stranded RNA mycovirus from fusarium graminearum. Appl. Environ. Microbiol. 68, 2529–2534. https://doi.org/10.1128/AEM.68.5.2529-2534.2002.

Cross, S.T., Maertens, B.L., Dunham, T.J., Rodgers, C.P., Brehm, A.L., Miller, M.R., Williams, A.M., Foy, B.D., Stenglein, M.D., 2020. Partitiviruses infecting Drosophila melanogaster and Aedes aegypti exhibit efficient biparental vertical transmission. J. Virol. https://doi.org/10.1128/JVI.01070-20.

Edgar, R.C., 2004. MUSCLE: multiple sequence alignment with high accuracy and high throughput. Nucleic Acids Res. 32, 1792–1797. https://doi.org/10.1093/nar/gkh340.

Fisher, M.C., Hawkins, N.J., Sanglard, D., Gurr, S.J., 2018. Worldwide emergence of resistance to antifungal drugs challenges human health and food security. Science 360, 739–742. https://doi.org/10.1126/science.aap7999.

Ghabrial, S.A., Castón, J.R., Jiang, D., Nibert, M.L., Suzuki, N., 2015. 50-plus years of fungal viruses. Virology 479–480, 356–368. https://doi.org/10.1016/j.virol.2015.02.034, 60th Anniversary Issue.

Gilbert, K.B., Holcomb, E.E., Allscheid, R.L., Carrington, J.C., 2019. Hiding in plain sight: new virus genomes discovered via a systematic analysis of fungal public transcriptomes. PLoS One 14, e0219207. https://doi.org/10.1371/journal.pone.0219207.

Gioti, A., Stajich, J.E., Johannesson, H., 2013. Neurospora and the dead-end hypothesis: genomic consequences of selfing in the model genus. Evolution 67, 3600–3616. https://doi.org/10.1111/evo.12206.

Gonçalves, C., Wisecaver, J.H., Kominek, J., Oom, M.S., Leandro, M.J., Shen, X.-X., Opulente, D.A., Zhou, X., Peris, D., Kurtzman, C.P., Hittinger, C.T., Rokas, A., Gonçalves, P., 2018. Evidence for loss and reacquisition of alcoholic fermentation in a fructophilic yeast lineage. eLife 7, e33034. https://doi.org/10.7554/eLife.33034.

Herrero, N., 2016. A novel monopartite dsRNA virus isolated from the entomopathogenic and nematophagous fungus Purpureocillium lilacinum. Arch. Virol. 161, 3375–3384. https://doi.org/10.1007/s00705-016-3045-y.

Hoang, D.T., Chernomor, O., von Haeseler, A., Minh, B.Q., Vinh, L.S., 2018. UFBoot2: improving the ultrafast bootstrap approximation. Mol. Biol. Evol. 35, 518–522. https://doi.org/10.1093/molbev/msx281.

Huang, Y.-W., Hu, C.-C., Lin, N.-S., Hsu, Y.-H., 2010. Mimicry of molecular pretenders: the terminal structures of satellites associated with plant RNA viruses. RNA Biol. https://doi.org/10.4161/rna.7.2.11089.

Ikeda, K., Inoue, K., Kida, C., Uwamori, T., Sasaki, A., Kanematsu, S., Park, P., 2013. Potentiation of mycovirus transmission by zinc compounds via attenuation of heterogenic incompatibility in Rosellinia necatrix. Appl. Environ. Microbiol. 79, 3684–3691. https://doi.org/10.1128/AEM.00426-13.

Kalyaanamoorthy, S., Minh, B.Q., Wong, T.K.F., von Haeseler, A., Jermiin, L.S., 2017. ModelFinder: fast model selection for accurate phylogenetic estimates. Nat. Methods 14, 587–589. https://doi.org/10.1038/nmeth.4285.

Kamaruzzaman, M., He, G., Wu, M., Zhang, J., Yang, L., Chen, W., Li, G., 2019. A novel partitivirus in the hypovirulent isolate QT5-19 of the plant pathogenic fungus Botrytis cinerea. Viruses 11, 24. https://doi.org/10.3390/v11010024.

Kerpedjiev, P., Hammer, S., Hofacker, I.L., 2015. Forna (force-directed RNA): simple and effective online RNA secondary structure diagrams. Bioinformatics 31, 3377–3379. https://doi.org/10.1093/bioinformatics/btv372.

Khankhum, S., Escalante, C., de Souto, E.R., Valverde, R.A., 2017. Extraction and electrophoretic analysis of large dsRNAs from desiccated plant tissues infected with plant viruses and biotrophic fungi. Eur. J. Plant Pathol. 147, 431–441. https://doi.org/10.1007/s10658-016-1014-7.

Kotta-Loizou, I., Coutts, R.H.A., 2017. Studies on the virome of the entomopathogenic fungus beauveria bassiana reveal novel dsRNA elements and mild hypervirulence. PLoS Pathog. 13 https://doi.org/10.1371/journal.ppat.1006183.

Krishnamurthy, S.R., Wang, D., 2018. Extensive conservation of prokaryotic ribosomal binding sites in known and novel picobirnaviruses. Virology 516, 108–114. https://doi.org/10.1016/j.virol.2018.01.006.

Langseth, W., 1998. Mycotoxin production and cytotoxicity of Fusarium strains isolated from Norwegian cereals. Mycopathologia 144, 103–113. https://doi.org/10.1023/A:1007016820879.

Lee, K.-M., Yu, J., Son, M., Lee, Y.-W., Kim, K.-H., 2011. Transmission of fusarium boothii mycovirus via protoplast fusion causes hypovirulence in other phytopathogenic Fungi. PLoS One 6, e21629. https://doi.org/10.1371/journal.pone.0021629.

Letunic, I., Bork, P., 2019. Interactive Tree of Life (iTOL) v4: recent updates and new developments. Nucleic Acids Res. 47, W256–W259. https://doi.org/10.1093/nar/gkz239.

Li, P., Bhattacharjee, P., Wang, S., Zhang, L., Ahmed, I., Guo, L., 2019. Mycoviruses in fusarium species: an update. Front. Cell. Infect. Microbiol. 9 https://doi.org/10.3389/fcimb.2019.00257.

Mahillon, M., Decroës, A., Liénard, C., Bragard, C., Legrève, A., 2019. Full genome sequence of a new polymycovirus infecting Fusarium redolens. Arch. Virol. https://doi.org/10.1007/s00705-019-04301-1.

Mahillon, M., Romay, G., Liénard, C., Legrève, A., Bragard, C., 2020. Description of a novel mycovirus in the phytopathogen fusarium culmorum and a related EVE in the yeast lipomyces starkeyi. Viruses 12, 523. https://doi.org/10.3390/v12050523.

McDonald, B.A., Stukenbrock, E.H., 2016. Rapid emergence of pathogens in agro-ecosystems: global threats to agricultural sustainability and food security. Philos. Trans. Biol. Sci. 371 https://doi.org/10.1098/rstb.2016.0026, 2016 0026.

Meena, N., Vasundhara, M., Reddy, M.S., Suravajhala, P., Raghavender, U.S., Medicherla, K.M., 2018. Draft genome sequence of a fungus (Fusarium tricinctum) cultured from a monoisolate native to the Himalayas. Genome Announc. 6 https://doi.org/10.1128/genomeA.00365-18.

Muhire, B.M., Varsani, A., Martin, D.P., 2014. SDT: a virus classification tool based on pairwise sequence alignment and identity calculation. PLoS One 9, e108277. https://doi.org/10.1371/journal.pone.0108277.

Nerva, L., Ciuffo, M., Vallino, M., Margaria, P., Varese, G.C., Gnavi, G., Turina, M., 2016. Multiple approaches for the detection and characterization of viral and plasmid symbionts from a collection of marine fungi. Virus Res. 219, 22–38. https://doi.org/10.1016/j.virusres.2015.10.028.

Nguyen, L.-T., Schmidt, H.A., von Haeseler, A., Minh, B.Q., 2015. IQ-TREE: a fast and effective stochastic algorithm for estimating maximum-likelihood phylogenies. Mol. Biol. Evol. 32, 268–274. https://doi.org/10.1093/molbev/msu300.

Nibert, M.L., Woods, K.M., Upton, S.J., Ghabrial, S.A., 2009. Cryspovirus: a new genus of protozoan viruses in the family Partitiviridae. Arch. Virol. 154, 1959–1965. https://doi.org/10.1007/s00705-009-0513-7.

Nibert, M.L., Tang, J., Xie, J., Collier, A.M., Ghabrial, S.A., Baker, T.S., Tao, Y.J., 2013. 3-d structures of fungal partitiviruses. Adv. Virus Res. 86, 59–85. https://doi.org/10.1016/B978-0-12-394315-6.00003-9.

Nibert, M.L., Ghabrial, S.A., Maiss, E., Lesker, T., Vainio, E.J., Jiang, D., Suzuki, N., 2014. Taxonomic reorganization of family Partitiviridae and other recent progress in partitivirus research. Virus Res. 188, 128–141. https://doi.org/10.1016/j.virusres.2014.04.007.

O'Donnell, K., Kistler, H.C., Tacke, B.K., Casper, H.H., 2000. Gene genealogies reveal global phylogeographic structure and reproductive isolation among lineages of Fusarium graminearum, the fungus causing wheat scab. Proc. Natl. Acad. Sci. U.S.A. 97, 7905–7910. https://doi.org/10.1073/pnas.130193297.

Proctor, R.H., McCormick, S.P., Kim, H.-S., Cardoza, R.E., Stanley, A.M., Lindo, L., Kelly, A., Brown, D.W., Lee, T., Vaughan, M.M., Alexander, N.J., Busman, M., Gutiérrez, S., 2018. Evolution of structural diversity of trichothecenes, a family of toxins produced by plant pathogenic and entomopathogenic fungi. PLoS Pathog. 14 https://doi.org/10.1371/journal.ppat.1006946.

Sabanadzovic, S., Valverde, R.A., Brown, J.K., Martin, R.R., Tzanetakis, I.E., 2009. Southern tomato virus: the link between the families Totiviridae and Partitiviridae. Virus Res. 140, 130–137. https://doi.org/10.1016/j.virusres.2008.11.018.

Sasaki, A., Miyanishi, M., Ozaki, K., Onoue, M., Yoshida, K., 2005. Molecular characterization of a partitivirus from the plant pathogenic ascomycete Rosellinia necatrix. Arch. Virol. 150, 1069–1083. https://doi.org/10.1007/s00705-005-0494-0.

Schneider, C.A., Rasband, W.S., Eliceiri, K.W., 2012. NIH Image to ImageJ: 25 years of image analysis. Nat. Methods 9, 671–675.

Shen, X.-X., Opulente, D.A., Kominek, J., Zhou, X., Steenwyk, J.L., Buh, K.V., Haase, M.A. B., Wisecaver, J.H., Wang, M., Doering, D.T., Boudouris, J.T., Schneider, R.M., Langdon, Q.K., Ohkuma, M., Endoh, R., Takashima, M., Manabe, R., Čadež, N., Libkind, D., Rosa, C.A., DeVirgilio, J., Hulfachor, A.B., Groenewald, M., Kurtzman, C.P., Hittinger, C.T., Rokas, A., 2018. Tempo and mode of genome evolution in the budding yeast subphylum. Cell 175, 1533–1545. https://doi.org/10.1016/j.cell.2018.10.023 e20.

Shi, M., Lin, X.-D., Tian, J.-H., Chen, L.-J., Chen, X., Li, C.-X., Qin, X.-C., Li, J., Cao, J.-P., Eden, J.-S., Buchmann, J., Wang, W., Xu, J., Holmes, E.C., Zhang, Y.-Z., 2016. Redefining the invertebrate RNA virosphere. Nature 540, 539–543. https://doi.org/10.1038/nature20167.

Shiba, K., Hatta, C., Sasai, S., Tojo, M., Ohki S, T., Mochizuki, T., 2018. Genome sequence of a novel partitivirus identified from the oomycete Pythium nunn. Arch. Virol. 163, 2561–2563. https://doi.org/10.1007/s00705-018-3880-0.

Song, Y., da Silva, N.M., Weiss, V.A., Vu, D., Moreno, L.F., Vicente, V.A., Li, R., de Hoog, G.S., 2020. Comparative genomic analysis of capsule-producing black yeasts exophiala dermatitidis and exophiala spinifera, potential agents of disseminated mycoses. Front. Microbiol. 11 https://doi.org/10.3389/fmicb.2020.00586.

Starr, E.P., Nuccio, E.E., Pett-Ridge, J., Banfield, J.F., Firestone, M.K., 2019. Metatranscriptomic reconstruction reveals RNA viruses with the potential to shape carbon cycling in soil. PNAS 116, 25900–25908. https://doi.org/10.1073/pnas.1908291116.

Sushida, H., Sumita, T., Higashi, Y., Iida, Y., 2019. Draft genome sequence of dicyma pulvinata strain 414-3, a mycoparasite of Cladosporium fulvum, causal agent of tomato leaf mold. Microbiol Resour Announc 8. https://doi.org/10.1128/MRA.00655-19.

Tang, J., Pan, J., Havens, W.M., Ochoa, W.F., Guu, T.S.Y., Ghabrial, S.A., Nibert, M.L., Tao, Y.J., Baker, T.S., 2010. Backbone Trace of Partitivirus Capsid Protein from Electron Cryomicroscopy and Homology Modeling. Biophys. J. 99, 685–694. https://doi.org/10.1016/j.bpj.2010.04.058.

Telengech, P., Hisano, S., Mugambi, C., Hyodo, K., Arjona-López, J.M., López-Herrera, C. J., Kanematsu, S., Kondo, H., Suzuki, N., 2020. Diverse partitiviruses from the phytopathogenic fungus, rosellinia necatrix. Front. Microbiol. 11 https://doi.org/10.3389/fmicb.2020.01064.

Urayama, S., Takaki, Y., Nishi, S., Yoshida-Takashima, Y., Deguchi, S., Takai, K., Nunoura, T., 2018. Unveiling the RNA virosphere associated with marine microorganisms. Mol. Ecol. Resour. 18, 1444–1455. https://doi.org/10.1111/17550998.12936.

Urayama, S., Doi, N., Kondo, F., Chiba, Y., Takaki, Y., Hirai, M., Minegishi, Y., Hagiwara, D., Nunoura, T., 2020. Diverged and active partitiviruses in lichen. Front. Microbiol. 11 https://doi.org/10.3389/fmicb.2020.561344.

Urban, M., Mott, E., Farley, T., Hammond-Kosack, K., 2003. The Fusarium graminearum MAP1 gene is essential for pathogenicity and development of perithecia. Mol. Plant Pathol. 4, 347–359. https://doi.org/10.1046/j.13643703.2003.00183.x.

Vainio, E.J., Korhonen, K., Tuomivirta, T.T., Hantula, J., 2010. A novel putative partitivirus of the saprotrophic fungus Heterobasidion ecrustosum infects pathogenic species of the Heterobasidion annosum complex. Fungal Biol. 114, 955–965. https://doi.org/10.1016/j.funbio.2010.09.006.

Vainio, E.J., Chiba, S., Ghabrial, S.A., Maiss, E., Roossinck, M., Sabanadzovic, S., Suzuki, N., Xie, J., Nibert, M., 2018. ICTV virus taxonomy profile: partitiviridae. J. Gen. Virol. 99, 17–18. https://doi.org/10.1099/jgv.0.000985.

Wang, L., Jiang, J., Wang, Y., Hong, N., Zhang, F., Xu, W., Wang, G., 2014. Hypovirulence of the phytopathogenic fungus Botryosphaeria dothidea: association with a coinfecting chrysovirus and a partitivirus. J. Virol. 88, 7517–7527. https://doi.org/10.1128/JVI.00538-14.

Waterhouse, A.M., Procter, J.B., Martin, D.M.A., Clamp, M., Barton, G.J., 2009. Jalview Version 2–a multiple sequence alignment editor and analysis workbench. Bioinformatics 25, 1189–1191. https://doi.org/10.1093/bioinformatics/btp033.

Wu, L.-P., Du, Y.-M., Xiao, H., Peng, L., Li, R., 2020. Complete genomic sequence of tea-oil camellia deltapartitivirus 1, a novel virus from Camellia oleifera. Arch. Virol. 165, 227–231. https://doi.org/10.1007/s00705-019-04429-0.

Xavier, A., da, S., Barros, A.P.Ode, Godinho, M.T., Zerbini, F.M., Souza, F., de, O., Bruckner, F.P., Alfenas-Zerbini, P., 2018. A novel mycovirus associated to Alternaria alternata comprises a distinct lineage in Partitiviridae. Virus Res. 244, 21–26. https://doi.org/10.1016/j.virusres.2017.10.007.

Xiao, X., Cheng, J., Tang, J., Fu, Y., Jiang, D., Baker, T.S., Ghabrial, S.A., Xie, J., 2014. A novel partitivirus that confers hypovirulence on plant pathogenic fungi. J. Virol. 88, 10120–10133. https://doi.org/10.1128/JVI.01036-14.

Xie, J., Jiang, D., 2014. New insights into mycoviruses and exploration for the biological control of crop fungal diseases. Annu. Rev. Phytopathol. 52, 45–68. https://doi.org/10.1146/annurev-phyto-102313-050222.

Yang, C., Hamel, C., Vujanovic, V., Gan, Y., 2011. Fungicide: modes of action and possible impact on nontarget microorganisms [WWW document]. ISRN Ecol. https://doi.org/10.5402/2011/130289.

Yao, Z., Zou, C., Peng, N., Zhu, Y., Bao, Y., Zhou, Q., Wu, Q., Chen, B., Zhang, M., 2020. Virome identification and characterization of fusarium sacchari and F. andiyazi: causative agents of pokkah boeng disease in sugarcane. Front. Microbiol. 11 https://doi.org/10.3389/fmicb.2020.00240.

Yinda, C.K., Ghogomu, S.M., Conceição-Neto, N., Beller, L., Deboutte, W., Vanhulle, E., Maes, P., Van Ranst, M., Matthijnssens, J., 2018. Cameroonian fruit bats harbor divergent viruses, including rotavirus H, bastroviruses, and picobirnaviruses using an alternative genetic code. Virus Evol. 4 https://doi.org/10.1093/ve/vey008.

Yu, X., Li, B., Fu, Y., Xie, J., Cheng, J., Ghabrial, S.A., Li, G., Yi, X., Jiang, D., 2013. Extracellular transmission of a DNA mycovirus and its use as a natural fungicide. Proc. Natl. Acad. Sci. U.S.A. 110, 1452–1457. https://doi.org/10.1073/pnas.1213755110.

Zhang, X., Xie, Y., Zhang, F., Sun, H., Zhai, Y., Zhang, S., Yuan, H., Zhou, L., Gao, F., Li, H., 2019. Complete genome sequence of an alternavirus from the phytopathogenic fungus Fusarium incarnatum. Arch. Virol. 164, 923–925. https://doi.org/10.1007/s00705-018-04128-2.

Zhang, C.J., Zhou, X.Y., Zhong, J., Guo, J., Yang, X.P., Zhu, H.J., 2020. Complete nucleotide sequence of a novel partitivirus infecting the plant-pathogenic fungus Phomopsis vexans. Arch. Virol. https://doi.org/10.1007/s00705-020-04835-9.

Zheng, L., Zhang, M., Chen, Q., Zhu, M., Zhou, E., 2014. A novel mycovirus closely related to viruses in the genus Alphapartitivirus confers hypovirulence in the phytopathogenic fungus Rhizoctonia solani. Virology 456–457, 220–226. https://doi.org/10.1016/j.virol.2014.03.029.

Zoll, J., Verweij, P.E., Melchers, W.J.G., 2018. Discovery and characterization of novel Aspergillus fumigatus mycoviruses. PLoS One 13, e0200511. https://doi.org/10.1371/journal.pone.0200511.

Zuker, M., 2003. Mfold web server for nucleic acid folding and hybridization prediction. Nucleic Acids Res. 31, 3406–3415. https://doi.org/10.1093/nar/gkg595.